Swarm Level 2 Processing System

Intermediate validation of Swarm Level 2 Core Field Product

SW_OPER_MCO_SHAi2C_20131125T000000_20190101T000000_0501

By: DTU

Date: 2019-02-22

Abstract and Conclusion

The processes and tests applied in the intermediate validation of the MCO_SHAi2C product

SW_OPER_MCO_SHAi2C_20131125T000000_20190101T000000_0501

and the conclusions on the product quality drawn herefrom are described in this document.

This product contains the representation of a model of the magnetic field of Earth's core and its temporal evolution ("MCO" part of product name) using spherical harmonic coefficients ("SHA" part of product name). The model is estimated from Swarm and ground observatory data using the *Comprehensive Inversion* (CI) scheme within the Swarm Level 2 Processing system ("2C" part of product name). Operational Swarm Level 1b data version 0505/0506, covering the period from 2013-11-25 to 2018-12-31 are used for the model estimation and the product is valid over the same period ("20131125T000000_20190101T000000" part of product name). This is version 0501 of the product (last part of product name), i.e. baseline 05 indicating 5th year CI production, first, minor version. The format of the product is described in "Product Specification for L2 Products and Auxiliary Products", doc. no. SW-DS-DTU-GS-0001.

The assessment of the SW_OPER_MCO_SHAi2C_20131125T000000_20190101T000000_0501 product shows very good agreement with recent versions of the CHAOS-6 model, [Finlay et.al., EPS, 2016].

The DTU SIL's opinion is that the MCO_SHAi2C product is successfully validated and therefore suitable for release.

Table of Contents

Table of Figures

Table of Tables

Abbreviations

Acronym	*Description*
CI	Comprehensive Inversion
CIY4	Comprehensive Inversion, Year 4
CIY5	Comprehensive Inversion, Year 5
CMB	Core-Mantle Boundary
L2PS	Level 2 Processing System
MCO	Magnetic Core field
SHA	Spherical Harmonic Analysis
SIL	Scientist in the Loop
STR	Star Tracker
VAL	Validation
VFM	Vector Field Magnetometer

References

[Finlay et.al., EPS, 2016] *Recent geomagnetic secular variation from Swarm and ground observatories as estimated in the CHAOS-6 geomagnetic field model*; Finlay, Christopher C.; Olsen, Nils; Kotsiaros, Stavros; Gillet, Nicolas; Tøffner-Clausen, Lars; Earth Planets and Space, Vol 68, 112 (2016). doi: 10.1186/s40623-016-0486-1

[Livermore et.al., NGEO, 2017] *An accelerating high-latitude jet in Earth's core*; Livermore, P.W., Hollerbach, R. and Finlay, C.C.; Nature Geoscience, 10, 62-68 (2017), doi:10.1038/ngeo2859

[Sabaka et.al., GRL, 2016] *Extracting Ocean-Generated Tidal Magnetic Signals from Swarm Data through Satellite Gradiometry*; Sabaka, Terence J. ; Tyler, Robert H. ; Olsen, Nils, Geophysical Research Letters (ISSN: 0094-8276, 2016), doi: 10.1002/2016GL068180

[Sabaka et.al., EPS, 2018] *A Comprehensive Model of Earth's Magnetic Field Determined From 4 Years of Swarm satellite observations*; Sabaka, Terence J. ; Tøffner-Clausen, Lars; Olsen, Nils; Finlay, Christopher C. Earth Planets and Space, in preparation.

1 Intermediate Validation Report of MCO_SHAi2C

1.1 Input data products

The following input data products were used for the estimation of the MCO_SHAi2C core field model

Products	Type	Period	Comment
SW_OPER_Q3D_CI_i2__00000000T000000_99999999T999999_0101	Q-matrix of Earth's (1-D mantle + oceans)	-	Used for computing induced part of ionospheric field
SW_OPER_AUX_OBS_2__20130101T000000_20131231T235959_0117 SW_OPER_AUX_OBS_2__20140101T000000_20141231T235959_0117 SW_OPER_AUX_OBS_2__20150101T000000_20151231T235959_0117 SW_OPER_AUX_OBS_2__20160101T000000_20161231T235959_0117 SW_OPER_AUX_OBS_2__20170101T000000_20171231T235959_0117 SW_OPER_AUX_OBS_2__20180101T000000_20181231T235959_0117	Observatory hourly mean values	2013-11-25 – 2017-10-31	A total of 163 observatories are included
SW_OPER_AUX_DST_2__19980101T013000_20190115T233000_0001 SW_OPER_AUX_F10_2__20060101T000000_20190115T000000_0001 SW_OPER_AUX_KP__2__19990101T023000_20190117T133000_0001	Indices	As indicated by the file names	
SW_OPER_MAGA_LR_1B_*yyyymmddTh1m1s1_yyyymmddTh2m2s2_vvvv* SW_OPER_MAGB_LR_1B_*yyyymmddTh1m1s1_yyyymmddTh2m2s2_vvvv* SW_OPER_MAGC_LR_1B_*yyyymmddTh1m1s1_yyyymmddTh2m2s2_vvvv*	Swarm magnetic data, 1 Hz	2013-11-25 - 2018-12-31	Decimated to 30 second sampling *vvvv* = 0505 or 0506

Table 1-1: Input data products

1.2 Model Parameterization and Data Selection

See Section 2.1.

1.3 Output Products

The products of this validation report are:

Swarm Level 2 Magnetic core field Product:

SW_OPER_MCO_SHAi2C_20131125T000000_20190101T000000_0501

Swarm Level 2 Intermediate Validation Product:

SW_OPER_MCO_VALi2C_20131125T000000_20190101T000000_0501

1.4 Validation Results

The tests were conducted between 2019-01-15 and 2019-02-10.

This 5th year CI L2 production, denoted CIY5, is very similar in methodology and results as last year's production (CIY4) which is thoroughly described in [Sabaka et.al., EPS, 2018]. The following contains the results of the tests performed on the core field product. See Annex A for general definitions of various tests.

1.4.1 Spatial Power Density

Figure 1-1 below shows the spatial power density of, a) the core field model (CIY5, solid blue line), b) the difference in the core field between the CIY5 and the CHAOS-6 resp. CIY4 models (dashed resp. dotted blue lines), c) the secular variation of the core field model (solid orange line), d) the difference in the core field secular variation between the CIY5 and CHAOS-6 resp. CIY4 models (dashed resp. dotted orange lines), e) the secular acceleration of the CIY5, CHAOS-6, CIY4 core field models (solid lines, green, cyan, and red respectively).

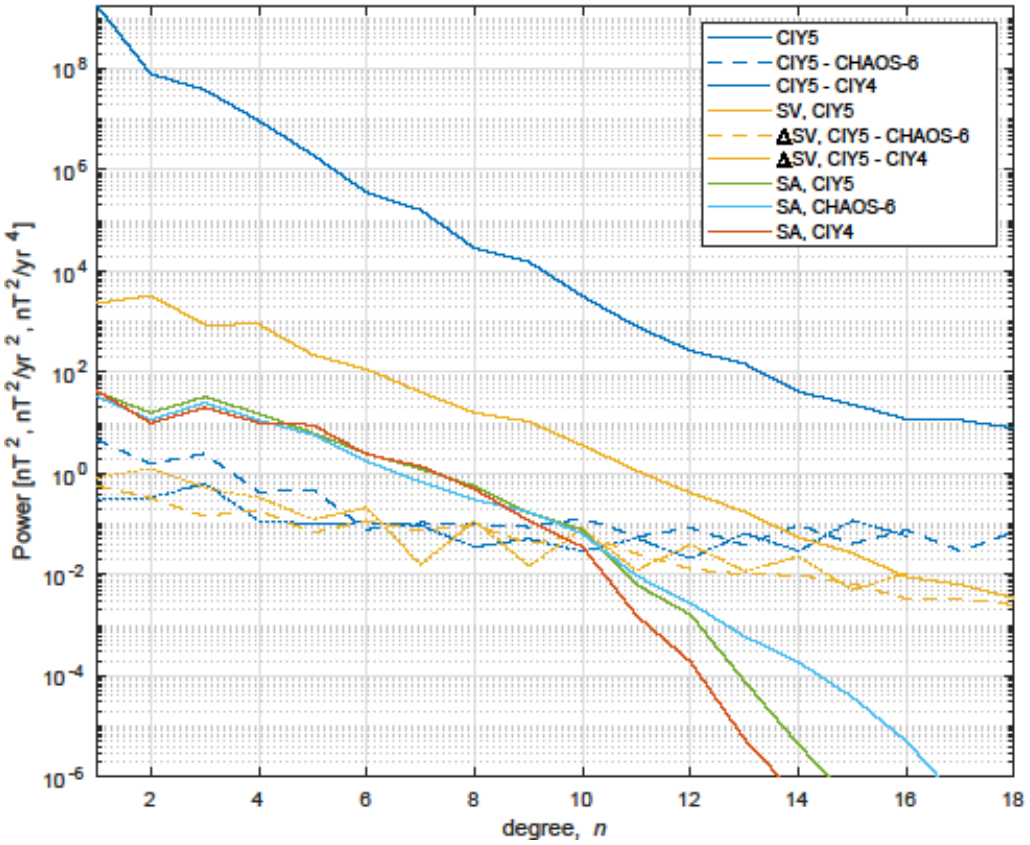

Figure 1-1: Spatial power densities, core field, epoch 2015

The CIY5 and the CHAOS-6 models agree very well for both the core field and its secular variation, and for the secular acceleration up to degree 12 where the power in the CIY5 model decreases significantly faster than the CHAOS-6 model indicating a heavy damping of the higher order secular acceleration in the CIY5 model. Note that the differences between CIY5 and CHAOS-6 respectively CIY4 are very similar indicating that the differences between the models are stochastic. Note also that the power of the secular acceleration has increased from CIY4 to CIY5 for spherical harmonic degrees above 10.

1.4.2 Secular Variation per Spherical Harmonic Coefficient

Figure 1-2 below shows timeseries of the first time-derivatives of the spherical harmonic coefficients up to degree 3. The red curves show the CIY5 core field model coefficient derivatives and the blue curves show the CHAOS-6 model coefficient derivatives. The figure confirms the good agreement between the two models.

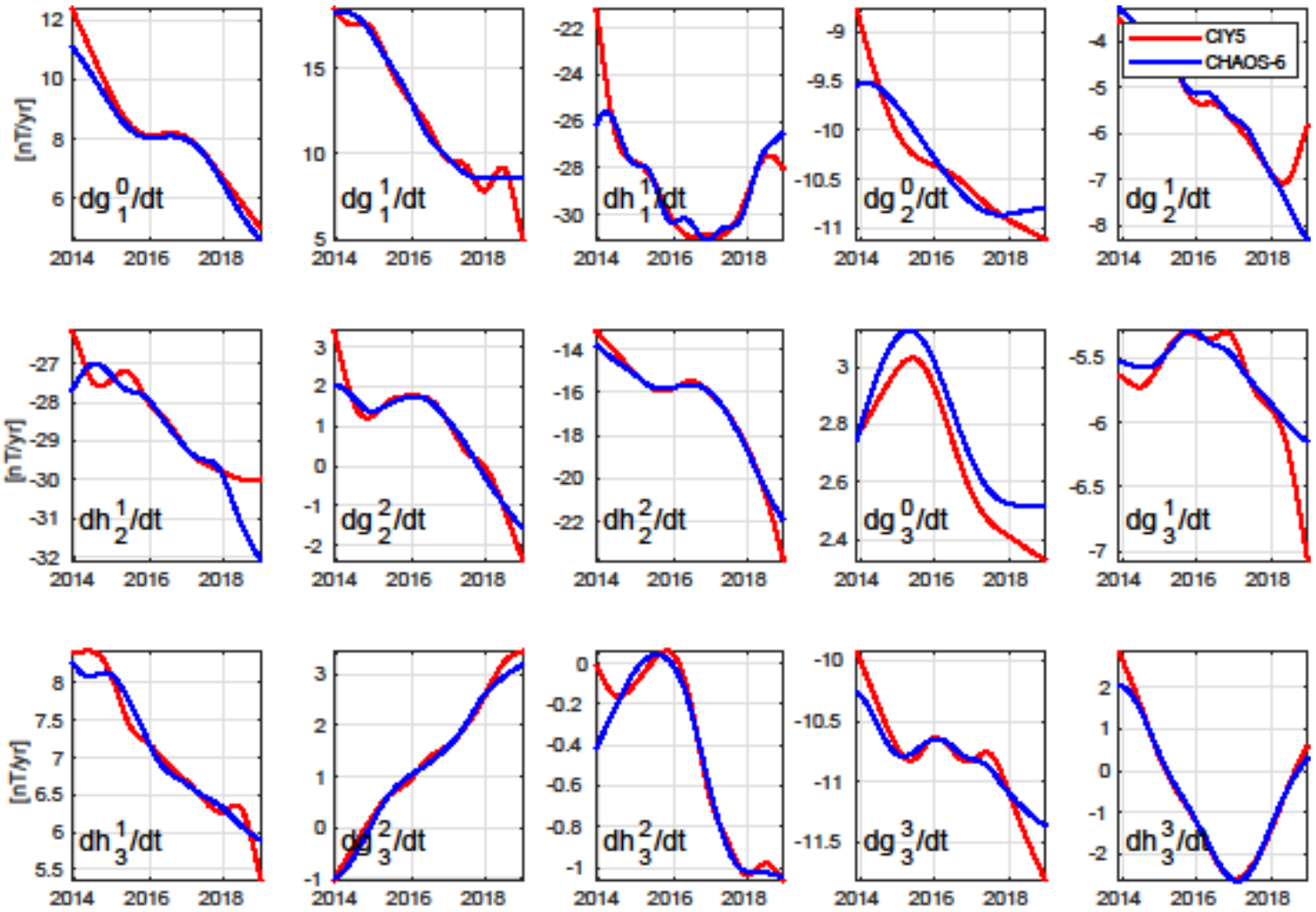

Figure 1-2: Time series of spherical harmonic coefficients, degrees 1-3

1.4.3 Secular Variation at Core-Mantle Boundary

Examining the vertical component of the magnetic field at the core-mantle boundary (CMB) show features similar to those found in CHAOS-6, [Livermore et.al., NGEO, 2017].

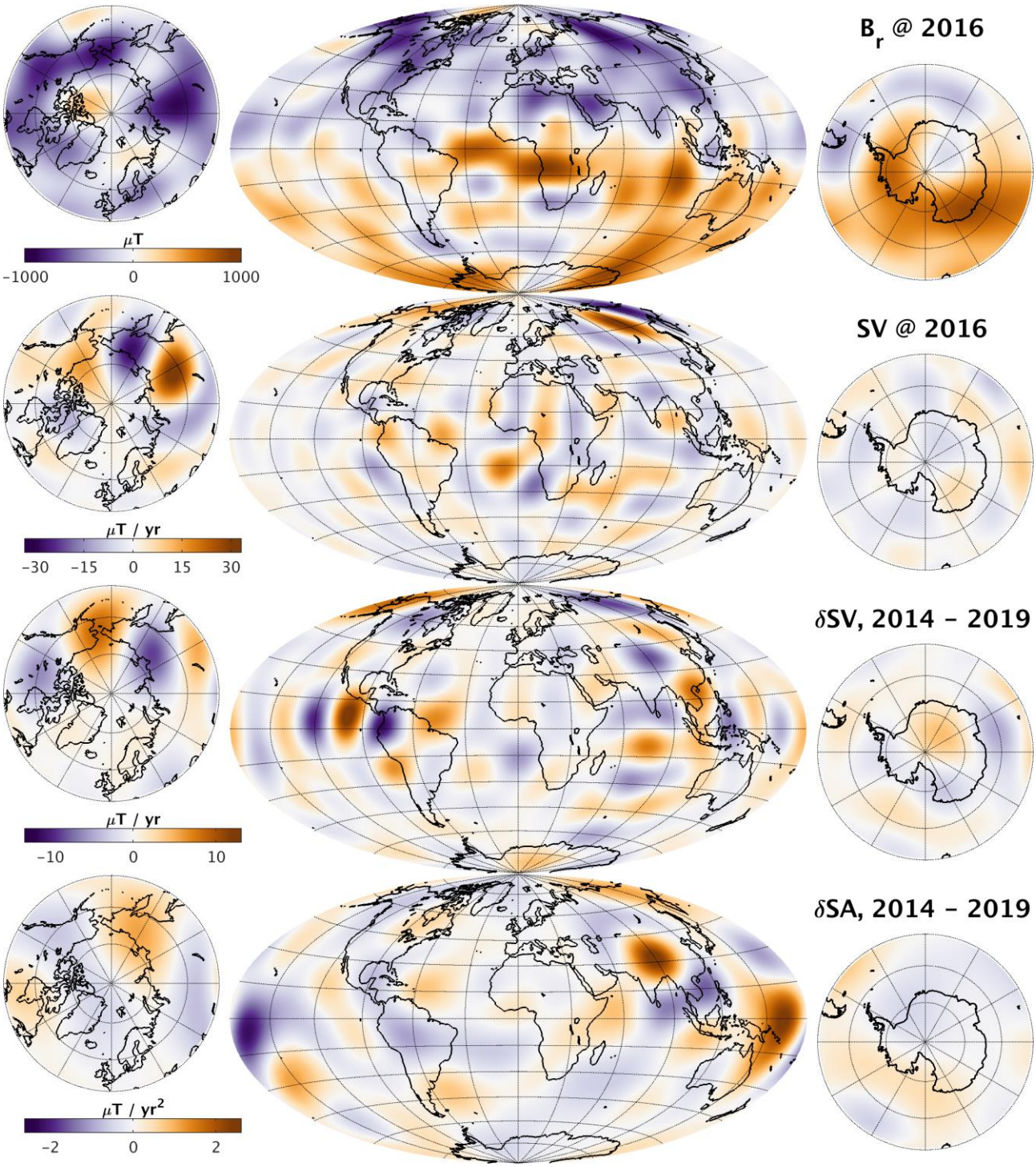

Figure 1-3 Maps of B_r and its changes at core-mantle boundary, up to degrees 13

Figure 1-3 above shows maps at the core-mantle boundary (CMB) of B_r and dB_r/dt ("SV") at epoch 2016, and of the changes in dB_r/dt ("δSV") and d^2B_r/dt^2 ("δSA") from 2014 to 2019.The structures in these maps are very similar to those found in CHAOS-6, only the signals in the time-varying fields near the South pole albeit small are probably affected by contamination from external, polar current systems and should be interpreted with caution.

1.4.4 Statistics of Model Residuals

The statistics of the data residuals obtained by the CIY5 modelling are given in Table 1-2 below. Grey cells indicate data from eclipse, white cells indicate data from sunlit regions. Crossed cells indicate data which are not used in the inversion process. "Field" indicate the pure vector and scalar measurements, whereas "NS diff" and "EW diff" indicate the North-South (along-track) respectively East-West differences ("gradients"). The standard deviations (of the residuals between the observations and the estimated model) of the differences are quite impressive; the standard deviations of the direct field measurements from the satellites are also remarkably. Note also the almost perfect similarity between Swarm A and C (side-by-side flying pair) and North-South differences for all three satellites. Swarm B shows slightly higher residuals in the horizontal and scalar Field components (B_θ, B_φ, and F) at low and mid latitudes and slightly lower residuals at high latitudes likely due to its higher altitude.

Swarm/Obs.		Geomagnetic quasi-dipole latitude											
		Low, ≤ 10°				Mid,]10°..55°]				High, > 55°			
		Standard deviations of data residuals, weighted, [nT]											
		$\sigma(B_r)$	$\sigma(B_\theta)$	$\sigma(B_\varphi)$	$\sigma(F)$	$\sigma(B_r)$	$\sigma(B_\theta)$	$\sigma(B_\varphi)$	$\sigma(F)$	$\sigma(B_r)$	$\sigma(B_\theta)$	$\sigma(B_\varphi)$	$\sigma(F)$
A	Field	1.63	1.92	1.66	2.41	1.65	2.09	2.07	1.78				5.62
	NS diff	0.31	0.18	0.32	0.16	0.24	0.28	0.35	0.18				0.93
		0.89	0.76	0.79	0.68	0.49	0.53	0.82	0.31				1.05
B	Field	1.64	2.49	1.98	3.29	1.88	2.55	2.26	2.33				5.44
	NS diff	0.30	0.18	0.30	0.16	0.24	0.28	0.34	0.19				0.83
		0.80	0.67	0.72	0.60	0.47	0.52	0.80	0.29				0.95
C	Field	1.64	1.87	1.64	2.38	1.65	2.08	2.07	1.78				5.62
	NS diff	0.32	0.18	0.32	0.16	0.25	0.29	0.35	0.18				0.93
		0.90	0.76	0.78	0.68	0.49	0.54	0.82	0.31				1.05
A-C	EW diff	0.55	0.40	0.74	0.36	0.38	0.44	0.75	0.32				0.55
		1.22	0.63	1.79	0.51	0.70	0.75	1.50	0.44				0.59
Magnetic observatories		3.99	4.01	4.50	n.c.	3.44	3.87	4.31	n.c.	13.23	12.83	10.41	n.c.
		11.41	13.43	9.39	n.c.	5.31	6.75	7.97	n.c.	16.26	17.37	15.07	n.c.

Table 1-2: Statistics of model residuals

1.5 Criteria

Table 1-3 below summarizes the criteria used to check the validity of the MCO_SHAi2C product.

Input	Test	Criteria	Pass?
Observations	Residual statistics	Standard deviation of vector data below 7 nT.	Ok
Alternative model	Comparison with model	CI model agrees with alternative model	Ok

Table 1-3: Validation criteria

2 Additional Information

2.1 Model Configuration and Data Selection Parameters

The MCO_SHAi2C product is obtained as a comprehensive co-estimation of the core, lithosphere, lunar M2 tidal, ionosphere, and magnetosphere field contributions including induced contributions similar to the method described in [Sabaka et.al., GRL, 2016]. The complete model configuration used is given in Table 2-1 below; the MCO_SHAi2C product is the green part:

Model Part	Maximum Degree/Order	Temporal Characteristics	Comment
Core	18/18	Order 5 B-spline with knots every 6 months	Damping of the mean-square, second and third time derivatives of B_r at the core-mantle boundary (at 3480 km radius) with enhanced damping of zonal terms up to degree 9.
Lithosphere	120/120	Static	Degree 19-120 purely determined by North-South differences from all satellites and East-West differences of lower pair satellite (A and C). Damping of B_r for degrees 91 and above to reduce noise
Ionosphere	45/5 (dipole coordinates)	Annual, semi-annual, 24-, 12-, 8- and 6- hours periodicity	Spherical harmonic expansion in quasi-dipole (QD) frame, underlying dipole SH $n_{max} = 60$, $m_{max} = 12$. Scaling by 3-months averages of F10.7 plus induction via a priori 3-D conductivity model ("1-D + oceans") and infinite conductor at depth. Damping of: 1. Mean-square current density J in the E-region within the nightside sector (magnetic local times 21:00 through 05:00; peak damping at 01:00) 2. Mean-square of the surface Laplacian of J multiplied by a factor of $\sin^8(2\theta)$ over all local times, where θ is co-latitude.

Model Part	Maximum Degree/Order	Temporal Characteristics	Comment
Magnetosphere, external	3/1	One hour bins	
Magnetosphere, induced	3/3	One hour bins	
M2 Tidal	18/18	Periodicity: 12.42060122 hr, phase fixed with respect to 00:00:00, 1999 January 1 GMT	

Table 2-1: Model Configuration

The data selection criteria are:

- Coarse agreement with CHAOS-6 field model: $\Delta B_c \leq 500$ nT for all components $c=r,\vartheta,\varphi$, and $\Delta F \leq 100$ nT.
- $Kp \leq 3^0$ for gradient data, $Kp \leq 2^-$ for field data
- Time-derivative of Dst: $|dDst/dt| \leq 3$ nT/hour
- 30 second satellite sampling period, NS gradient data computed from 15 second differences
- core and tidal fields determined from night-side data only, i.e. with Sun $\geq 10°$ below the horizon

2.2 Comments from Scientists in the Loop

2.2.1 Derivation of Model

The final Comprehensive Inversion model using five years of Swarm data shows good agreement with alternative model and excellent statistics (Table 1-2), although caution must be taken when studying time-varying features at the core-mantle boundary (Section 1.4.3).

2.2.2 Conclusion

The estimated model is assessed to be of good quality with well-behaved characteristics and very good agreement with alternative core field model.

Annex A Definitions of Tests

A.1 Mean square vector field difference per spherical harmonic degree

The mean square vector field difference between models per spherical harmonic degree (n) is diagnostic of how closely the models match on average across the globe. The difference between Gauss coefficients ${}^{m}_{n}g$ of model i and model j can be defined as:

$$ {}_{i,j}R_n = (n+1)\left(\frac{a}{r}\right)^{(2n+4)} \sum_{m=0}^{n}\left[{}_{i}g_n^m - {}_{j}g_n^m\right]^2 $$

Equation A-1

where n is the degree, m is the order, a is the magnetic reference spherical radius of 6371.2 km which is close to the mean Earth radius, and r is the radius of the sphere of interest, which is taken as r = a for comparisons at the Earth's surface and r = 3480 km for comparisons at the core-mantle boundary.

Summing over degrees n from 1 to the truncation degree N and taking the square root yields the RMS vector field difference between the models i and j averaged over the spherical surface:

$$ {}_{i,j}R = \sqrt{\sum_{n=1}^{N} {}_{i,j}R_n} $$

Equation A-2

A.2 Correlation per spherical harmonic degree

Analysis of spherical harmonic spectra is a powerful way to diagnose differences in amplitude between models but tells us little about how well they are correlated. The correlation per degree between two models again labelled by the indices i and j can be studied as a function of spherical harmonic degree using the quantity: ${}_{i,j}\rho_n$

$$ {}_{i,j}\rho_n = \frac{\sum_{m=0}^{n}\left({}_{i}g_n^m \; {}_{j}g_n^m\right)}{\sqrt{\left(\sum_{m=0}^{n}\left({}_{i}g_n^m\right)^2\right)\left(\sum_{m=0}^{n}\left({}_{j}g_n^m\right)^2\right)}} $$

Equation A-3

Ideally, the correlation should be close to 1 for all models, indicating that they have equivalent features and coefficients. If the correlation falls below 0.5, for degrees 1-9, then the models should be examined in more detail. Coefficients from degree 10-13 in IGRF and WMM are less well-determined (e.g. due to noise) and also change more rapidly so are not expected to be well correlated by the launch of the Swarm mission.

A.3 Visualisation of coefficient differences

A final method of visualising the differences in Gauss coefficients is to plot the differences ${}_{i}g_n^m - {}_{j}g_n^m$ as a triangular plot, with the zonal coefficients lying along the centre of the triangle, the sectorial coefficients along the edges and the tesseral coefficients filling the central regions. These plots will illustrate which, if any, coefficients are strongly divergent between models.